

Note on convergence of MFS in the disc

Alex H. Barnett

June 26, 2006

Abstract

We analyze convergence rate and coefficient sizes needed in the MFS (a particular case of the MPS) for Dirichlet's problem for Laplace's equation in the disc. This answers most of Timo's questions in Memo 1 of 27/10/05. We also investigate the continuous limit of MFS in more general shapes by studying the SVD of the single layer operator from the outer to inner boundary.

1 Problem and definitions

Let Ω be the unit disc in $\mathbb{R}^2 = \mathbb{C}$. We wish to solve

$$\Delta u = 0 \quad \text{in } \Omega \quad (1)$$

$$u = f \quad \text{on } \partial\Omega \quad (2)$$

where $f \in C(\partial\Omega)$ is a real function. Generally the MPS approximates

$$u \approx u^{(N)} = \sum_{j=0}^{N-1} \alpha_j \xi_j \quad (3)$$

where $\alpha_j \in \mathbb{R}$ are coefficients and ξ_j are real 'basis' (trial) functions. Coords will be written $x = re^{i\theta}$. Traditional MPS uses harmonic monomials,

$$\xi_j(x) = \begin{cases} 1, & j = 0 \\ r^j \cos j\theta, & 0 < j \leq (N+1)/2 \\ r^{j-(N+1)/2} \sin[j - (N+1)/2]\theta, & (N+1)/2 < j < N \end{cases} \quad (4)$$

Here the case of N odd is given; the highest sin or cos must be dropped if N is even.

The fundamental solution is $E(x, y) = -\frac{1}{2\pi} \ln |x - y|$ for $x, y \in \mathbb{C}$. The MFS is a special case of the MPS. Given an outer radius $R > 1$, MFS uses the point charges

$$\xi_j(x) = E(x, y_j) \quad \text{for } 0 \leq j < N, \quad (5)$$

where $y_j = Re^{i\phi_j}$ are at uniformly-spaced angles $\phi_j = 2\pi j/N$, see Fig. 1.

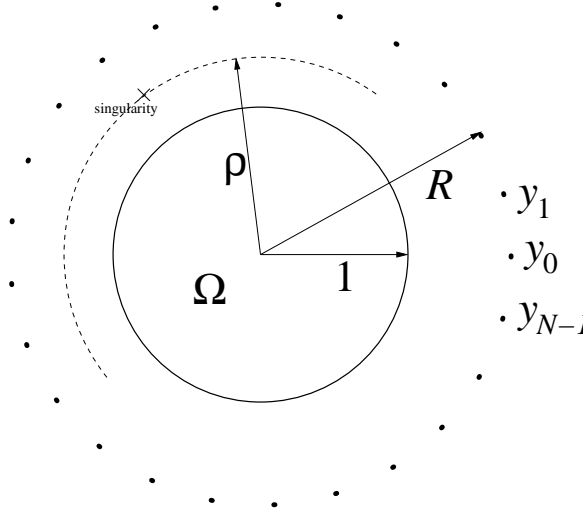


Figure 1: Geometry for MFS in the disc.

Now the vector of coefficients $\{\alpha_j\}_{0 \leq j < N} =: \boldsymbol{\alpha} \in \mathbb{R}^N$ is determined by minimizing the L^2 -norm of the boundary error,

$$t(\boldsymbol{\alpha}) := \|u^{(N)} - f\|_{L^2(\partial\Omega)}. \quad (6)$$

Call the minimum achieved t_0 , and the coefficient vector which achieves this minimum $\boldsymbol{\alpha}_0$. Fixing a particular boundary function f of norm $O(1)$, we may ask, in exact arithmetic,

- how does t_0 depend on N ?
- how does $|\boldsymbol{\alpha}_0|$ depend on N ?

In practise, (6) is minimized by discretizing the boundary integral in (6) using M quadrature points. This gives a linear algebra least-squares problem of the form $\min_{\boldsymbol{\alpha}} |A\boldsymbol{\alpha} - \mathbf{f}|$, where $\mathbf{f} \in \mathbb{R}^M$. This can be solved via SVD. The rectangular matrix A has entries of the form $A_{kj} = \sqrt{w_k} \xi_j(x_k)$, where $\{x_k\}_{k=1, \dots, M}$ are a set of quadrature points and $\{w_k\}$ the corresponding weights. We note that some authors have chosen $M = N$ but we find this unnecessarily restrictive and unmotivated.

Remark 1 *The crucial practical limitation is that $|\boldsymbol{\alpha}_0| < 1/\epsilon_{mach}$ since otherwise relative errors due to round-off in $u^{(N)}$ become $O(1)$. A key question is then, how small can t_0 be at the N at which $|\boldsymbol{\alpha}_0| \approx 1/\epsilon_{mach}$? We might instead allow N to be larger than this but choose $\boldsymbol{\alpha} \neq \boldsymbol{\alpha}_0$. This may involve a regularization scheme.*

Now some definitions. Any $g \in L^2(\partial\Omega)$ may be written in the Fourier basis,

$$g(\theta) = \sum_{m=-\infty}^{\infty} \hat{g}(m) e^{im\theta}, \quad \hat{g}(m) = \frac{1}{2\pi} \int_{S^1} g(\theta) e^{-im\theta} d\theta, \quad (7)$$

where $\theta \in \partial\Omega = S^1 = [0, 2\pi)$. This relies on the elementary result

$$\int_{S^1} e^{im\theta} d\theta = 2\pi \delta_{m0} \quad (8)$$

where δ_{mn} is the Kronecker delta. Parseval's relation is

$$\|g\|_2^2 = 2\pi \sum_{m=-\infty}^{\infty} |\hat{g}(m)|^2. \quad (9)$$

2 Map from layer potential to Fourier basis

It is worth first considering a simpler problem. The single layer potential lying on the outer circle $\partial\Omega_R$, where $\Omega_R := \{x : |x| \leq R\}$, is

$$u(x) = \int_{S^1} E(x, Re^{i\phi}) g(\phi) d\phi. \quad (10)$$

Note $g \in L^1(S^1)$ is the density with respect to angle measure $d\phi$ rather than the usual length measure $Rd\phi$. This layer potential is the $N \rightarrow \infty$ limit of MFS. The polynomial decomposition of a fundamental solution located at $Re^{i\phi}$ is (following Katsurada)

$$\begin{aligned} E(x, Re^{i\phi}) &= -\frac{1}{2\pi} \ln |Re^{i\phi} - x| \\ &= -\frac{1}{2\pi} \operatorname{Re} \ln(Re^{i\phi} - x) \\ &= -\frac{1}{2\pi} \left[\ln R + \operatorname{Re} \ln \left(1 - \frac{r}{R} e^{i(\theta-\phi)} \right) \right] \\ &= -\frac{1}{2\pi} \left[\ln R - \sum_{m \in \mathbb{Z}, m \neq 0} \frac{1}{2|m|} \left(\frac{r}{R} \right)^{|m|} e^{im(\theta-\phi)} \right]. \end{aligned} \quad (11)$$

Note that this represents a real function of x . The restriction of (10) to $x \in \partial\Omega$ is an operator $S : L^2(S^1) \rightarrow L^2(S^1)$ which takes g to $u|_{\partial\Omega}$. It is a convolution, therefore diagonal in the Fourier basis $\{e^{im\theta}\}_{m \in \mathbb{Z}}$. Comparing (11), (10) and using (8) gives $\hat{u}(m) = \hat{s}(m) \hat{g}(m)$ where the operator's eigenvalues are

$$\hat{s}(m) = \begin{cases} -\ln R, & m = 0 \\ \frac{1}{2|m|} R^{-|m|}, & m \neq 0 \end{cases} \quad (12)$$

Since its kernel $E(e^{i\cdot}, Re^{i\cdot})$ is continuous the operator is compact, reflected by $\lim_{|m| \rightarrow \infty} \hat{s}(m) = 0$.

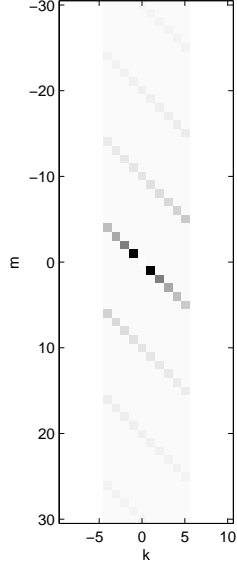


Figure 2: Density plot of matrix elements (18) for $N = 10$, in the domain $|m| \leq 30$. We chose the small value $R = 1.01$ in order to make the super- and sub-diagonals more visible (for more typical R they are exponentially small).

Remark 2 *The compactness of S means its inverse is unbounded, and we expect to find arbitrarily large densities $\|g\|$ needed to represent unit-norm boundary values $u|_{\partial\Omega}$.*

Remark 3 *S is reminiscent of the Poisson kernel $P : L^2(S^1) \rightarrow L^2(S^1)$ which given u harmonic in Ω_R takes $u|_{\partial\Omega_R}$ to $u|_{\partial\Omega}$. This is also diagonal in the Fourier basis with eigenvalues*

$$\hat{p}(m) = \begin{cases} 1, & m = 0 \\ R^{-|m|}, & m \neq 0 \end{cases} \quad (13)$$

and is also compact.

3 Map from MFS coefficients to Fourier basis

We now adapt the above to the discrete case. By using

$$g(\phi) = \sum_{j=0}^{N-1} \alpha_j \delta(\phi - \phi_j) \quad (14)$$

in (10) we recreate the MFS representation $u^{(N)}$ of (3), (5). From now we choose N even. We represent coefficients in a discrete Fourier basis labeled by

$$-N/2 < k \leq N/2,$$

$$\alpha_j = \sum_{k=-N/2+1}^{N/2} \hat{\alpha}_k e^{ik\phi_j}, \quad \hat{\alpha}_k = \frac{1}{N} \sum_{j=0}^{N-1} \alpha_j e^{-ik\phi_j}, \quad (15)$$

where inversion follows from $\sum_{j=0}^{N-1} e^{2\pi i k j / N} = N \delta_{k0}^{(N)}$, where the periodized Kronecker delta is

$$\delta_{kj}^{(N)} = \begin{cases} 1, & k \equiv j \pmod{N} \\ 0, & \text{otherwise.} \end{cases} \quad (16)$$

We define the operator $T : \mathbb{R}^N \rightarrow l^2(\mathbb{Z})$ which takes the discrete Fourier coefficient vector $\{\hat{\alpha}_k\}_{-N/2 < k \leq N/2} =: \hat{\alpha}$ to the boundary Fourier coefficient vector $\{\hat{u}(m)\}_{m \in \mathbb{Z}}$. It is bounded for the following reason: since the map (15) is bounded, $g \in L^1(S^1)$, and $S : L^1(S^1) \rightarrow L^2(S^1)$ is bounded, finally (9) holds. The action of T is then that of an ∞ -by- N matrix:

$$\hat{u}(m) = \sum_{k=-N/2+1}^{N/2} t_{mk} \hat{\alpha}_k, \quad \text{for } m \in \mathbb{Z}. \quad (17)$$

Proposition 1 *In terms of the definitions (12) and (16), the matrix elements of T are*

$$t_{mk} = \frac{N}{2\pi} \hat{s}(m) \delta_{mk}^{(N)}. \quad (18)$$

Proof: We define $m \bmod N$ to lie in the range $-N/2+1, \dots, N/2$. The Fourier series representation of (14) is $\hat{g}(m) = (1/2\pi) \sum_{j=0}^{N-1} \alpha_j e^{-im\phi_j} = (N/2\pi) \hat{\alpha}_{m \bmod N}$, for $m \in \mathbb{Z}$, where the last step used (15). The diagonal representation of S gives $(T\hat{\alpha})(m) = (\widehat{Sg})(m) = \hat{s}(m) \hat{g}(m)$, which completes the proof. \square

Fig. 2 shows a greyscale picture of a piece of the resulting matrix t_{mk} . Notice that it is dominated by a main diagonal proportional to the diagonal of the S operator defined in (12), but with (exponentially) smaller entries on an infinite sequence of super- and sub-diagonals. This off-diagonal part can be interpreted as ‘sampling overtones’ due to discretization of a continuous layer potential.

4 Error estimates and coefficient sizes for MFS approximation

The above gives a Fourier matrix representation of the MFS basis. Using (17) and (9) gives the boundary error (6) in terms of discrete Fourier coefficients as

$$t(\hat{\alpha}) = \sqrt{2\pi} |T\hat{\alpha} - \hat{f}| \quad (19)$$

where $\hat{f} \in l^2(\mathbb{Z})$ is the vector of Fourier coefficients of f . Minimizing this is a least-squares problem involving the matrix T . Since T is nearly diagonal

(apart from in its extreme columns), we will pretend it is diagonal in order to come up with vectors $\hat{\alpha}$ that are sufficiently close to the true least-squares solution. This corresponds to approximating polynomial MPS by MFS. Thus we cannot significantly beat the triangle inequality used by Bogomolny (and Timo). However, by returning to the properties of the matrix T (each column can be treated in isolation since they live in orthogonal subspaces) we could beat this inequality, although I feel gains would be small in the disc due to small off-diagonal elements size (and because MPS is perfectly adapted to the disc).

We will use the following simple l^2 bound on the off-diagonal part of the n^{th} column of T .

Lemma 1 *Let $n \in \mathbb{Z}$, $-N/2 < n \leq N/2$, then*

$$\sum_{b \neq 0} \hat{s}(bN + n)^2 \leq \frac{R^{-2N+2|n|}}{2(N - |n|)^2(1 - R^{-2N})} \quad (20)$$

Proof: Consider $n \geq 0$. The sum consists of super- and sub-diagonal contributions,

$$\sum_{b > 0} \frac{R^{-2bN-2n}}{4(bN + n)^2} + \sum_{b < 0} \frac{R^{2bN+2n}}{4(bN + n)^2} \leq \frac{1}{4(N - n)^2} (R^{-2n} + R^{2n}) \sum_{b > 0} (R^{-2N})^b$$

which summing the geometric series and bounding the sum of powers of R completes the proof. The answer for $-n$ is identical to that for n by symmetry of $\hat{s}(m)$. \square

Later we care only about the exponential part, so we have

Corollary 1 *Assume $R^{2N} \geq 2$, then*

$$\sum_{b \neq 0} \hat{s}(bN + n)^2 \leq R^{-2N+2|n|} \quad (21)$$

4.1 A single MPS particular solution

Lemma 2 *Fix N an even positive integer, let $f = e^{in\theta}$, with $n \in \mathbb{Z}$, $|n| \leq N/2$, and let $R > 1$. Then the minimum value of the MFS boundary error (6) satisfies*

$$t_0 \leq \begin{cases} \sqrt{\frac{\pi}{1 - R^{-2N}}} \frac{1}{N} \frac{R^{-N}}{\ln R}, & n = 0 \\ \sqrt{\frac{\pi}{1 - R^{-2N}}} \frac{2|n|}{N - |n|} R^{-N+2|n|}, & n \neq 0 \end{cases} \quad (22)$$

Proof: Let $\mathbf{e}^{(n)}$ be the unit vector with 1 in the n^{th} entry. Then $\hat{\mathbf{f}} = \mathbf{e}^{(n)}$. We use coefficients $\hat{\alpha} = t_{nn}^{-1} \mathbf{e}^{(n)}$. For any n , (19) gives

$$\begin{aligned} t(\hat{\alpha})^2 &= 2\pi |T\hat{\alpha} - \mathbf{e}^{(n)}|^2 \\ &= 2\pi \sum_{m \neq n} |(T\hat{\alpha})(m)|^2 \\ &= 2\pi \sum_{b \neq 0} \frac{t_{bN+n,n}^2}{t_{nn}^2} = \frac{2\pi}{\hat{s}(n)^2} \sum_{b \neq 0} \hat{s}(bN+n)^2 \end{aligned} \quad (23)$$

Inserting (12) for the cases $n = 0$ or $n \neq 0$ and using Lemma 1 completes the proof. Note that $n = -N/2$ has the same MFS coefficients as $n = N/2$ so is equivalent. \square

Corollary 2 *The bounds of Lemma 2 hold with the replacement $f = \sin n\theta$ or $f = \cos n\theta$.*

This is similar to Bogomonly's result Eq. (3.9), and his method of proof. (he omits the $n = 0$ case - why?). I don't think this is new, just simpler.

Note that the worst-approximated Fourier modes are near $\pm N/2$, with $n = \pm N/2$ having $O(1)$ errors.

Remark 4 *The coefficient vector required grows exponentially, with 2-norm $|\alpha| = \sqrt{N} t_{nn}^{-1} = 2\sqrt{N} |n| R^{|n|}$. Here we used discrete Parseval $|\alpha|^2 = N |\hat{\alpha}|^2$.*

4.2 Function harmonic in a larger disc

If u satisfying (1), (2) is continuable to a function harmonic in Ω_ρ for some $\rho > 1$, this is equivalent to exponential decay of Fourier coefficients

$$|\hat{f}(m)| \leq C \rho^{-|m|}. \quad (24)$$

An example is Timo's single pole $u(z) = \text{Re}(z - a)^{-1}$ with $\rho = a$.

Theorem 1 *For real analytic boundary data obeying (24), the minimum error achievable with the MFS with given $R > 1$ and N even, with $R^{2N} \geq 2$, satisfies,*

$$t_0 \leq \begin{cases} C \rho^{-N/2}, & \rho < R^2 \\ C N R^{-N}, & \rho = R^2 \\ C R^{-N}, & \rho > R^2 \end{cases} \quad (25)$$

where each time C means different constants independent of f and N .

Proof: We choose coefficients $\hat{\alpha}_m = \hat{f}(m)/\hat{s}(m)$, $\forall m \in \mathbb{Z}$ in order to exactly match the Fourier coefficients in the domain $-N/2 < m \leq N/2$. Therefore

errors are due only to frequencies outside this domain. (19) and the triangle inequality give

$$t_0 = \left(2\pi \sum_{m \notin [-\frac{N}{2}+1, \frac{N}{2}]} |(T\hat{\alpha})(m) - \hat{f}(m)|^2 \right)^{1/2} \leq \sqrt{2\pi}(E_u + E_f)$$

where

$$\begin{aligned} E_u^2 &= \sum_{m \notin [-\frac{N}{2}+1, \frac{N}{2}]} |(T\hat{\alpha})(m)|^2 = \sum_{-\frac{N}{2} < n \leq \frac{N}{2}} \left| \frac{\hat{f}(n)}{\hat{s}(n)} \right|^2 \sum_{b \neq 0} |\hat{s}(bN + n)|^2 \\ &\leq CR^{-2N} \sum_{-\frac{N}{2} < n \leq \frac{N}{2}} \left(\frac{R^2}{\rho} \right)^{2|n|}, \end{aligned} \quad (26)$$

where we used (24), Lemma 1, and $|n|/(N - |n|) \leq 1$, and

$$E_f^2 = \sum_{m \notin [-\frac{N}{2}+1, \frac{N}{2}]} |\hat{f}(m)|^2 \leq C\rho^{-N}. \quad (27)$$

We now study the sum in (26). For $\rho < R^2$, the series is growing so its sum is bounded by $C(R^2/\rho)^N$. This means both E_u^2 and E_f^2 can be estimated by $C\rho^{-N}$. For $\rho = R^2$, the series contains N equal terms of size unity. For $\rho > R^2$, the series decays so the sum is bounded by $O(1)$, which means E_f^2 is of higher order compared to E_u^2 and can be dropped. \square

This is analogous to a result in the sup norm proved by Katsurada (1989). It's therefore not really a new result. The choice of coefficients is not quite optimal but won't affect the exponential terms. The triangle inequality is not throwing away much in the proof since the elements of the two vectors are unlikely to be related to each other.

Remark 5 *In the two regimes convergence rate is controlled by different effects:*

1. *f is 'not very' analytic ($\rho < R^2$): errors limited by the absence of Fourier modes beyond a frequency $N/2$. In this case the MFS is well approximating the MPS, and has the same convergence rate.*
2. *f is 'very' analytic ($\rho > R^2$): errors limited by the errors due to discrete representation of the layer potential, as with Lemma 2. The MPS would do better than MFS.*

Note that the interesting case of singularity closer than R falls in the former category. This predicts Timo's observed rate 1.22^{-N} since $\rho^{1/2} = \sqrt{1.5} = 1.22 \dots$.

Remark 6 *Coefficient sizes are bounded by $|\hat{\alpha}_m| \leq C|m|(R/\rho)^{|m|}$. So in the case $\rho > R$, the singularity is outside the MFS source circle, coefficients die, and*

$|\alpha| \leq CN^{3/2}$ is quite weak polynomial growth. But in the interesting case $\rho < R$, coefficients grow exponentially and their norm is dominated by essentially the largest term, giving $|\alpha| \leq CN^{3/2}(R/\rho)^{N/2}$.

At what N do we expect convergence to cease? When the ratio between error size and coefficient size reaches $\epsilon_{\text{mach}}^{-1}$, roundoff error becomes equal in size to the approximation errors derived above, so errors cannot be expected to decrease any further. Let's try this in the above latter case $\rho < R$. Setting this ratio $(R/\rho)^{N/2}/\rho^{-N} = \epsilon_{\text{mach}}^{-1}$ gives $N = N_{\text{fail}} = 2 \log \epsilon_{\text{mach}}^{-1} / \log R$. In Timo's experiment $R = 2$, predicting $N_{\text{fail}} = 106$, which is very close to the observed value 90.

In conclusion, this answers some of Timo's questions of 27/10/05:

1. The asymptotic error estimate for MFS is optimal.
2. MFS is as fast as MPS.
3. Don't know yet!
4. Coefficient sizes have been explained, and a prediction made for when convergence stops which agrees quite well with the $N = 90$ found.

5 Domains other than a disc

We can say a lot using the continuous limit of MFS. In a general simply-connected domain Ω enclosed by a general Jordan curve $\partial\Omega^+$ the single layer operator is

$$u(x) = \int_{\partial\Omega^+} E(x, y) g(y) dy. \quad (28)$$

Restricting u to $\partial\Omega$ gives a 1D integral operator S such that $u|_{\partial\Omega} = Sg$. We desire $u|_{\partial\Omega}$ to approximate f in $L^2(\partial\Omega)$. We write the singular value decomposition of the operator as

$$S = \sum_{j=1}^{\infty} \sigma_j u_j(v_j, \cdot), \quad (29)$$

where $\sigma_1 \geq \sigma_2 \geq \dots \rightarrow 0$ since S is compact. The left singular vectors u_j are orthonormal in $L^2(\partial\Omega)$. Numerically the only functions on $\partial\Omega$ that we can represent with $o(1)$ error in the form Sg , for some g , are those in $\text{Span} \{u_j\}_{j=1, \dots, r}$. Here $r := \#\{j : \sigma_j/\sigma_1 > \epsilon_{\text{mach}}\}$ is the numerical rank.

Now we choose Ω^+ a much larger disc (radius 3-10, for Ω radius about 1 or less). This will also correspond to the case of MPS with polynomials or plane-wave basis. In Figs. 3, 4 and 5 and 6 we show left singular vectors as their harmonic extensions in Ω . Explicitly, (28) is plotted in Ω with the choice $g = v_j/\sigma_j$, for $j = 1, 2, \dots$. Thus the correctly-normalized u_j can be read off on the boundary. These are computed using non-uniformly weighted quadrature on $\partial\Omega$ and $\partial\Omega^+$, with a few hundred points, and the matrix SVD.

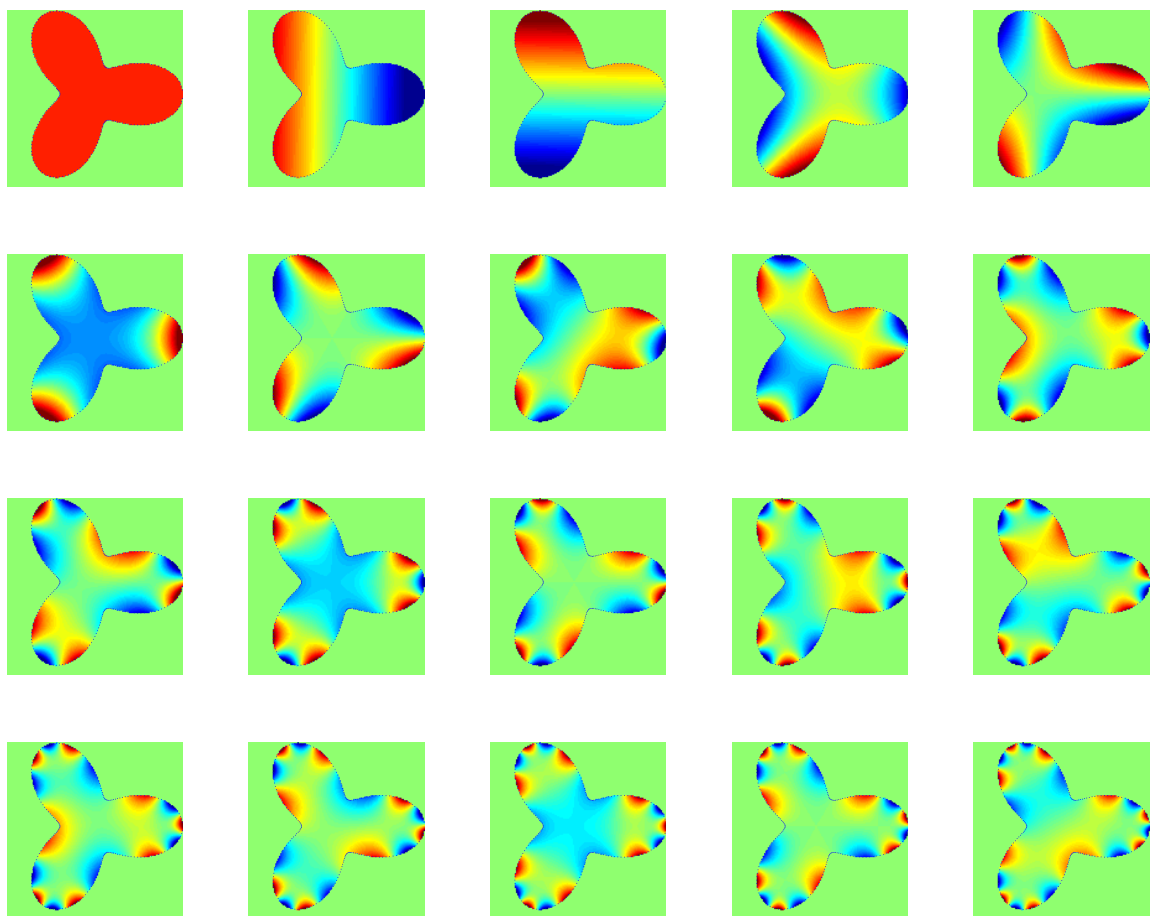


Figure 3: First 20 left singular vectors of S operator for Ω a trefoil domain, with outer boundary a large circle.

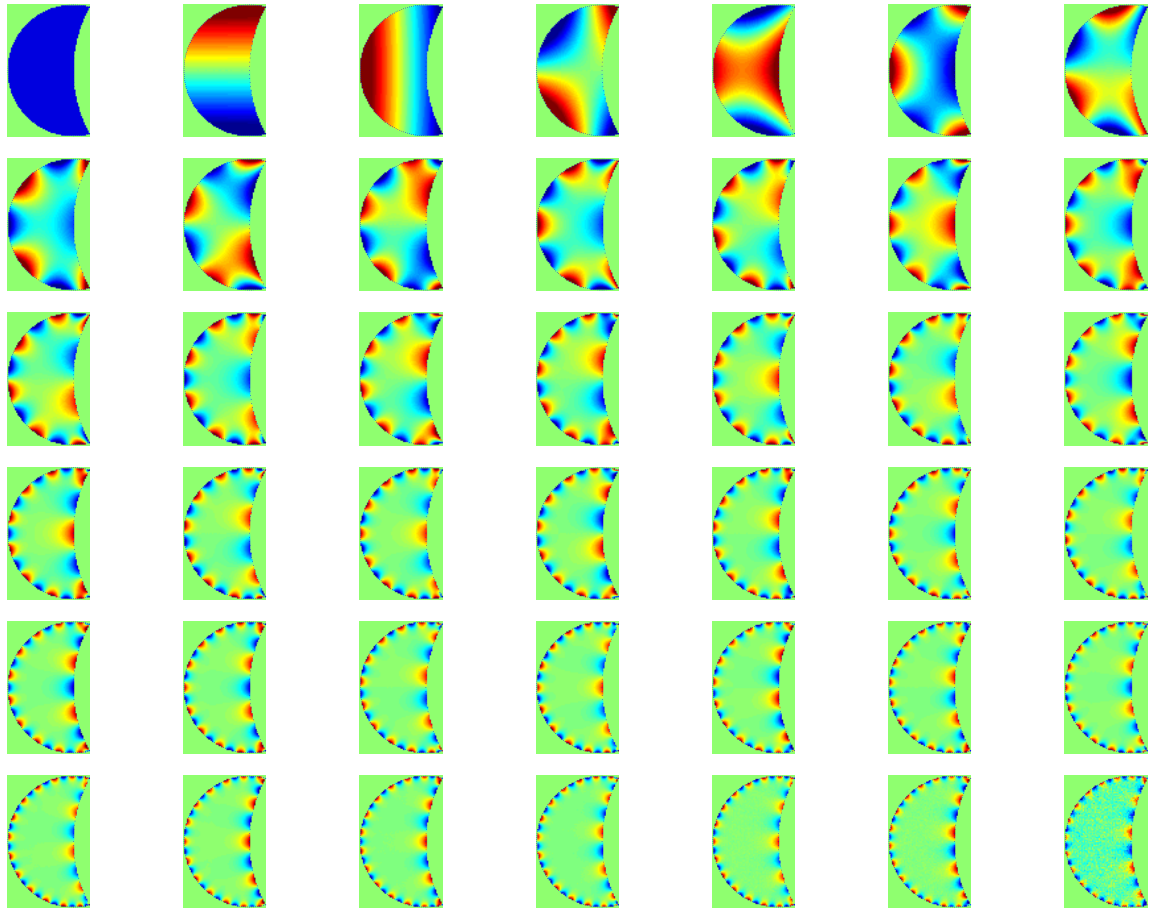


Figure 4: First 42 left singular vectors of S operator for Ω a purse domain, with outer boundary a large circle.

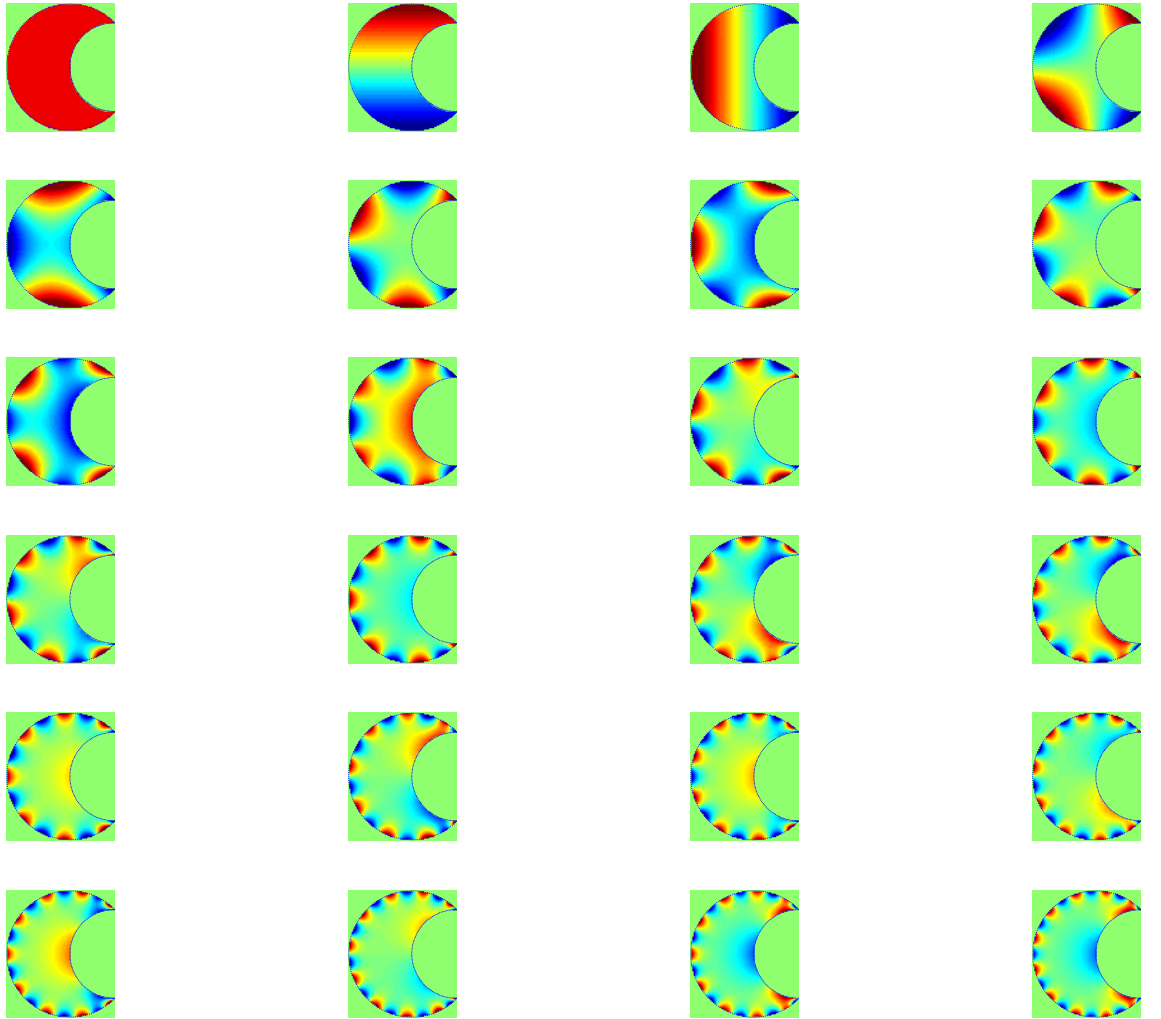


Figure 5: First 24 left singular vectors of S operator for Ω a crescent domain, with outer boundary a large circle.

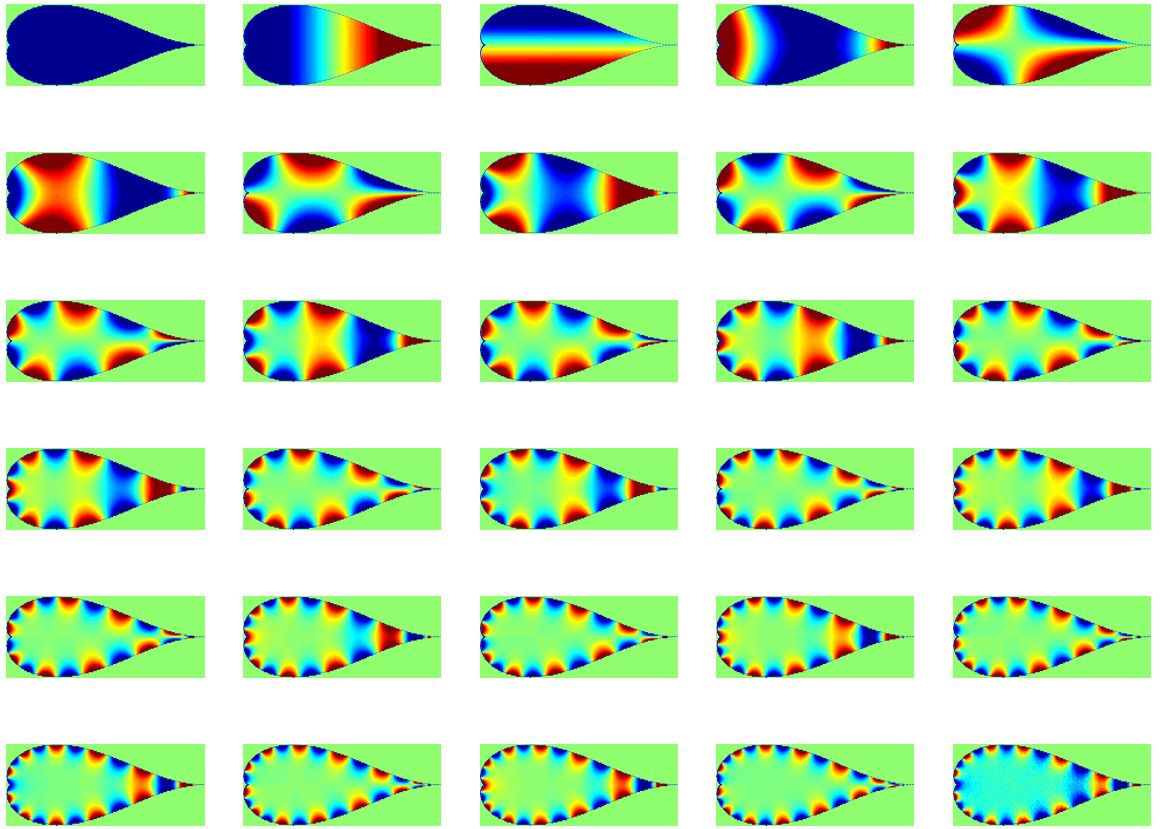


Figure 6: First 24 left singular vectors of S operator for Ω a droplet domain with an exterior cusp, with outer boundary a circle radius 3.

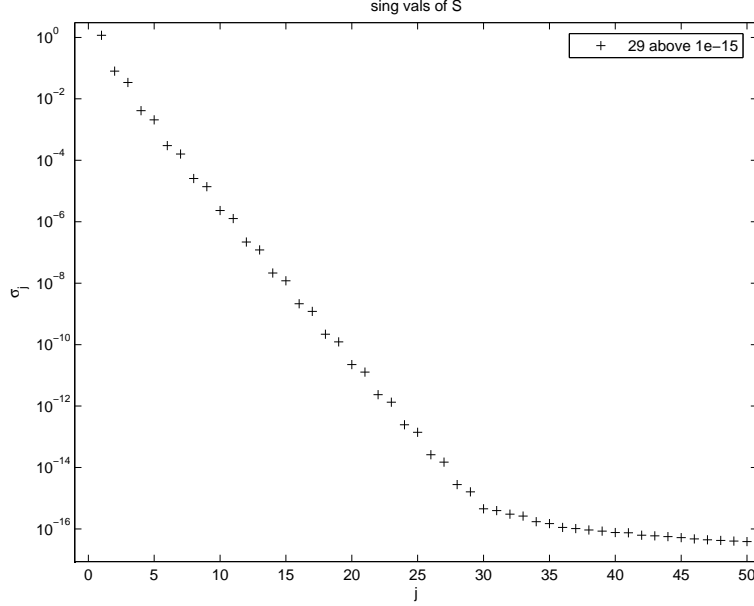


Figure 7: Singular values of droplet shape, for outer boundary a circle radius 3.

We now care only about the approximation properties of $\{u_j\}_{j=1,\dots,r}$ in $L_2(\partial\Omega)$, or whatever norm we wish to approximate f in. Notice that concave regions have very few oscillations in u_j , therefore it would be very hard to represent a function f with any interesting features in this region using this choice of Ω^+ . The right singular vectors v_j are pretty close to $\cos(j-1)\phi$ on $\partial\Omega^+$, therefore σ_j is dominated by the ratio of radii to the power $(j-1)$. Exponential decay of σ_j is apparent in Fig. 7.

Conjecture 1 *In the limit Ω^+ is a disc of radius $R \rightarrow \infty$, the right singular vectors v_j tend to the Fourier series on Ω^+ .*

Why? This follows from the fact that the circle Ω^+ is large, that is $R \gg 1$. This means the value of a n^{th} degree harmonic polynomial is dominated by $c_n R^n e^{in\phi}$, and that lower powers give relatively small contribution. Thus each singular vector v_j is close to z^n at large radii. This is illustrated by the right side of Fig. 8.

I'm hoping for something of the following nature, currently a bit fuzzy.

Conjecture 2 *In the limit Ω^+ is a disc of radius $R \rightarrow \infty$, the left singular vectors u_j tend to the Faber polynomials multiplied by $w^{-1/2}(x)$ where $w(x)$ is the weight function on $\partial\Omega$ which is conformally equivalent to uniform measure on the unit circle.*

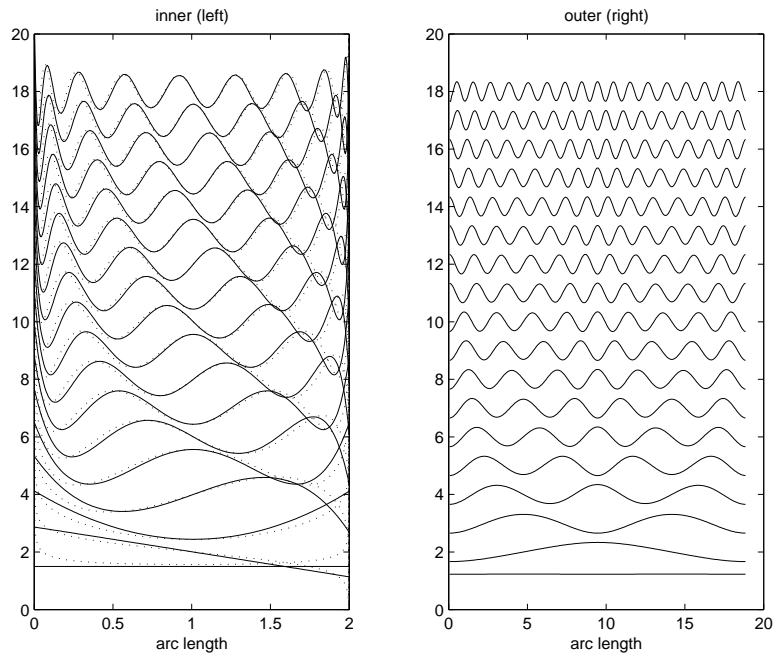


Figure 8: Left and right singular vectors (shown as solid lines) of $\Omega = [-1, 1]$, for outer boundary a circle radius 3. The dotted lines show the Chebyshev polynomials $w^{-1/2}(x)T_n(x)$ where their weight function is $w(x) = 1/\sqrt{1-x^2}$.

This is suggested by the right singular vectors tending to z_n and containing only nonnegative powers. They also could be conformally mapped to w^n where $z = \phi(w)$ in Curtiss 1977 notation. I believe this makes them Faber polynomials. Proof needs to be attempted. It is suggested by choosing a real interval as Ω (whose Faber poly's are the Chebychev poly's): Fig. 8 shows that u_j are very close to Chebychev poly's with the correct reweighting to make orthonormal with uniform measure on $[-1, 1]$. The roots do concentrate with expected square-root singularity. This contrasts with the initial guess by looking at Fig. 6 which seemed to show that no such concentration of roots occurs.

Conjecture 3 *In the limit Ω^+ is a disc of radius $R \rightarrow \infty$, the density of oscillations (roots) of u_j is given by the surface charge density of the equilibrium (constant potential) charge distribution on a conducting body in free space.*

Expect this to follow using density of zeros technique in Ch. 5 of Trefethen Spectral Methods book.

If $\partial\Omega^+$ is now not restricted to be a large circle, the left singular vectors are no longer Faber polynomials. Thus Faber polys are not much help for the MFS with $\partial\Omega^+$ not a circle - saves us learning about them!

Conjecture 4 *For general $\partial\Omega^+$ and $\partial\Omega$, the relevant potential problem whose surface charge gives the density of zeros of u_j on $\partial\Omega$ (and of v_j on $\partial\Omega^+$) is the 'coaxial' (if you're an electrical engineer) capacitor problem given by $\Delta u = 0$ in $\Omega^+ \setminus \overline{\Omega}$, $u|_{\partial\Omega} = 1$, $u|_{\partial\Omega^+} = 0$.*

This needs to be proven; it could be very useful for choosing MFS source distances. Need to look up asymptotics of orthog polys (note the weight function is always unity though). This immediately suggests that choosing constant distance from $\partial\Omega^+$ to $\partial\Omega$ is good since the zeros of u_j will be approx uniform on $\partial\Omega$, leading to good Fourier-like convergence in $L^2(\partial\Omega)$. This annular potential problem could be conformally mapped to the annulus, relates to Katsurada 1996.

This continuous model of MFS gives upper bounds on errors. We see that replacing (28) by the MFS corresponds to 'deleting columns' of the (discretized) operator S , and this cannot increase the singular values (can it? Know any theorem on this?).

Questions:

1. What kind of o.n.b. does $\text{Span } \{u_j\}_{j=1,\dots,r}$ form? Should it tell us that $\partial\Omega^+$ should be chosen with knowledge of f , not just Ω ?
2. How close should we bring $\partial\Omega^+$ to $\partial\Omega$? When close, MFS point density should be increased so that sampling errors discussed in previous Section do not dominate.
3. Can a version of the convergence Theorem in Ch. 5 of Trefethen *Spectral Methods in Matlab* be found for general domain and outer boundary shape? Expect it to rely on potential theory.

6 Discussion of previous results

Browder 1962: Thm 3 is the relevant, very surprising result, which says that if the PDE has the Cauchy unique continuation property (which Laplace, etc, do), then the MFS can approximate arbitrarily well any solution in any simply-connected domain G_1 , using only charges restricted to any other disjoint domain G_3 . This is done by proving that the subspace S_3 of solutions in G_1 generated by the MFS in G_3 is dense in the subspace S_1 of regular solutions in G_1 . This in turn is done by proving that $u \perp S_3 \Rightarrow u \perp S_1$. This is similar to Lax 1957, Mergelyan, etc. Of course no mention of coefficient sizes, which would be ridiculously large in practise. I have worked through this proof looking for a way to turn this into a useful inequality. I'm pretty sure nothing can be done, because unique continuation is exponentially unstable: Let u solve the PDE in a region enclosing both G_1 and G_3 . There is no constant C such that $\|u\|_{L^2(G_1)} \leq C\|u\|_{L^2(G_3)}$ neither the other way round (\geq). Either way round high-frequency evanescent waves are the culprit: they can have arbitrarily large growth or decay rates. So it's a practically useless theorem. The method of proof of Browder's Thm 3 is used by Bogomolny 1985 in the case of G_3 a curve enclosing G_1 .

Eisenstat (in Mathon + Johnson 1977): has theorem that MFS has potential to be exponentially convergent in the disc with *some* choice of charge locations. This is an elegant hack: the MFS coefficients are all forced to be unity, and the locations are the zeros of a polynomial approximating e^{u+iv} , where v is the harmonic conjugate of u . This allows known polynomial approximation results to carry over to MFS. The constant term is handled by another hack: that you can generate a sufficiently constant field by a sum of two opposing unit-strength charges a large distance from the disc.

Katsurada 1988: In case where exactly N collocation points are used, that is

$$t(\alpha) := \sqrt{\sum_{k=0}^{N-1} |u^{(N)}(x_k) - f(x_k)|^2} \quad (30)$$

where $x_k = e^{i\theta_k}$, Katsurada has proven MFS gives unique solution via a square matrix having nonzero determinant. This depends on the relative rotational offset of the source vs collocation points, which is not discussed. This is only useful if we want to set $M = N$ which I think is a distraction (the Greeks, Karageorghis, etc, do this a lot too). However Katsurada's ideas on i) Fourier analysis, and especially ii) conformal mapping (1994, 1996) for analytic boundary curve, are very interesting. He proves (1996) that the equivalent of my S operator between two general concentric curves is a relatively compact perturbation of S . Worth looking into.

Bogomolny 1985: too much squeezed into one paper.

7 Questions / thoughts

- The L^2 norm was used since that's what we care about in MPS for eigenvalue problems. We could have used sup norm.
- Should we investigate conformal mapping of the disc (and its uniformly-spaced sources) as Katsurada does? I have tried Driscoll's SC toolbox and verified the exponential 'crowding' problem is severe for high-aspect ratio domains for the internal disc map, but is only as severe as a square-root singularity for the external disc map (that Faber polys use). Katsurada uses the latter.
- My feeling is MFS with charges uniformly spaced in arclength will outperform MPS in elongated or highly nonconvex shapes. Would love us to test this.
- Generalize the above to other source types (dipole, ie simple pole, etc) is easy, just replace the Taylor series in (11). Generalize to Helmholtz equation requires Addition Thm (J_m expansion for Y_0 about the argument kR). Should not be hard. Ennenbach (1996) has already done it I think, so should dig it up.
- (Faber polynomials seem to be the right way to do MPS for Laplace's equation in a general shape, since they are orthonormal on $\partial\Omega$ I think. I found Curtiss 1971 excellent review. However, from what I can make out are a mess to calculate and are only known analytically for a few shapes. We don't want their calculation to be more complicated than the Dirichlet problem itself! Some approximate Faber might be good compromise. I am less interested in Faber because I care more about Helmholtz than Laplace in the end.) Obsolete question.
- (What are Faber poly's for Helmholtz equation?) Obsolete question.
- Here's a puzzler: consider Ω with maximum radius R from the origin, with boundary data corresponding to u having a singularity at distance $\rho < R$ from the origin. Does the usual MPS blow up at radius ρ , that is, fail to converge in the part of Ω lying outside the ρ -disc? If so, doesn't this violate the theorem that says polynomial approx converges in any Ω ? If not, doesn't this violate usual results about series diverging beyond radius of convergence? What am I missing here?